Handling Uncertainties Through Reliability-Based Optimization Using Evolutionary Algorithms

Kalyanmoy Deb*, Dhanesh Padmanabhan†, Sulabh Gupta‡and Abhishek Kumar Mall§

KanGAL Report Number 2006009

Abstract

Uncertainties in design variables and problem parameters are inevitable and must be considered in an optimization task, if reliable optimal solutions are to be found. Besides the sampling techniques, there exist a number of reliability-based probabilistic optimization techniques for systematically handling such uncertainties. In this paper, first we present a brief review of these classical probabilistic procedures. Thereafter, we discuss different optimization tasks in which these classical reliability-based optimization procedures will, in general, have difficulties in finding true optimal solutions. These probabilistic techniques are borrowed from classical literature and are extended to constitute efficient reliability-based single and multi-objective evolutionary algorithms for solving such difficult problems. Due to the global perspective of evolutionary algorithms, first, we demonstrate the proposed methodology is better able to solve reliability based optimization problems having multiple local-global solutions. Second, we suggest introducing an additional objective of maximizing the reliability index along with optimizing the usual objective function and find a number of Pareto-optimal solutions trading-off between the objective value and corresponding reliability index, thereby allowing the designers to find solutions corresponding to different reliability requirements for a better application. Finally, the concept of single-objective reliability-based optimization is extended to multi-objective optimization of finding a reliable frontier, instead of a single reliable solution. These optimization tasks are illustrated by solving a number of test problems and a well-studied automobile design problem. Results are also compared with a couple of standard classical reliability-based methodologies. This paper demonstrates how classical reliability-based concepts can be used in single and multi-objective evolutionary algorithms to enhance their scope in handling uncertainties, a matter which is common in most real-world problem solving tasks.

1 Introduction

For practical optimization studies, reliability-based techniques are getting increasingly popular, due to the uncertainties involved in realizing design variables and stochasticities involved in various problem parameters. For a canonical deterministic optimization task, the optimum solution usually lies on a constraint surface or at the intersection of more than one constraint surfaces. However, if the design variables or some system parameters cannot be achieved exactly and are

*Professor, Department of Mechanical Engineering, Indian Institute of Technology Kanpur, PIN 208016, India, Email: deb@iitk.ac.in (corresponding author)

†India Science Laboratory, GM R&D, Bangalore, PIN 560066, India, Email: dhanesh.padmanabhan@gm.com

‡Undergraduate Student, Department of Computer Science, Indian Institute of Technology Kanpur, PIN 208016, India, Email: sulabhg@iitk.ac.in

§Undergraduate Student, Department of Computer Science, Indian Institute of Technology Kanpur, PIN 208016, India, Email: akmall@iitk.ac.in

uncertain with a known probability distribution of variation, the deterministic optimum (lying on one or more constraint surfaces) will fail to remain feasible in many occasions. In such scenarios, a stochastic optimization problem is usually formed and solved, in which the constraints are converted into probabilistic constraints meaning that probability of failures (of being a feasible solution) is limited to a pre-specified value (say $(1 - R)$) [22, 9], where R is called the reliability of design.

Existing reliability-based optimization techniques vary from each other in the manner they handle the probabilistic constraints. One simple-minded approach would be to use a Monte-Carlo simulation technique to create a number of samples following the uncertainties and stochastitices in the design variables and problem parameters and evaluate them to compute the probability of failure [17, 2]. However, such a technique becomes computationally expensive when the desired probability of failure is very small. To alleviate this computational problem, more sophisticated sampling techniques are suggested.

Recently, optimization-based methodologies, instead of sampling methods, are suggested to take care of the probabilistic constraints. In these methods, stochastic variables and parameters are transformed into the standard normal variate space and a separate optimization problem is formulated to compute the largest probability of failure and equate it with the desired value. At least three different concepts – double-loop methods, single-loop methods and decoupled methods – have been followed. In this paper, we extend one of these concepts to be used with an evolutionary optimization technique. We apply the proposed methodology to three different types of optimization problems and demonstrate by solving test problems and an automobile design problem that the evolutionary optimization based reliability consideration is ideal for these problems. Results are compared with a couple of classical methods and merits and demerits of them are discussed. This paper clearly brings out problem domains in which reliability-based evolutionary algorithms will have an edge over their classical counterparts and should encourage more such studies.

2 Classical Reliability-Based Methodologies

We consider here a reliability-based single-objective optimization problem of the following type:

$$\begin{array}{lll} \underset{(\mathbf{x},\mathbf{d})}{\text{Minimize}} & f(\mathbf{x},\mathbf{d},\mathbf{p}), & \\ \text{Subject to} & g_j(\mathbf{x},\mathbf{d},\mathbf{p}) \geq 0, & j = 1,2,\ldots,J, \\ & h_k(\mathbf{d}) \geq 0, & k = 1,2,\ldots,K, \\ & \mathbf{x}^{(L)} \leq \mathbf{x} \leq \mathbf{x}^{(U)}, & \\ & \mathbf{d}^{(L)} \leq \mathbf{d} \leq \mathbf{d}^{(U)}. & \end{array} \tag{1}$$

Here, $\mathbf{x}$ is a set of design variables which are uncertain, $\mathbf{d}$ is a set of deterministic design variables, and $\mathbf{p}$ is a set of uncertain parameters (which are not design variables). Thus, the stochasticity in the optimization problem comes from two sets of variables: $\mathbf{x}$ and $\mathbf{p}$. Here, we only consider inequality constraints. This is because if an equality constraint involves $\mathbf{x}$ or $\mathbf{p}$, there may not exist a solution for any arbitrary desired reliability against failure. All inequality constraints can be classified into two categories: (i) stochastic constraints g_j involves at least one random variables ($\mathbf{x}$, $\mathbf{p}$ or both) and (ii) h_k involves no random variables.

Figure 1 shows a hypothetical problem with two stochastic inequality constraints. Typically, the optimal solution lies on a constraint boundary or at the the intersection of more than one constraints, as shown in the figure. In the event of uncertainties in design variables, as shown in the figure with a probability distribution around the optimal solution, in many instances such

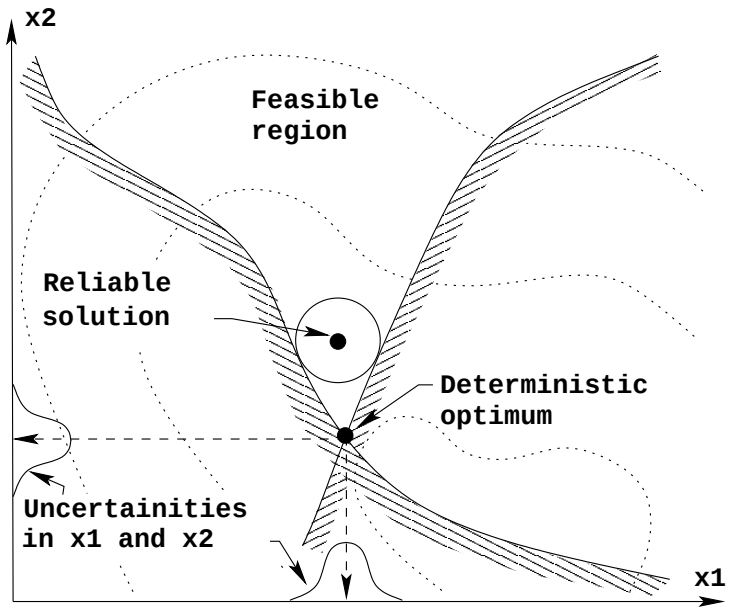

Figure 1: The concept of reliability-based optimization procedure is illustrated.

a solution will be infeasible. In order to find a solution which is more reliable (meaning that there is a very small probability of instances producing an infeasible solution), the true optimal solution must be sacrificed and a solution interior to the feasible region may be chosen. For a desired reliability measure R, it is then desired to find that feasible solution which will ensure that the probability of having an infeasible solution instance created through uncertainties from this solution is at most $(1 - R)$. To arrive at such a solution, the above optimization problem can be converted to a deterministic optimization problem. Since the objective function f and constraints g_j are also random due to the randomness in variables $\mathbf{x}$ and parameter $\mathbf{p}$, usually the following deterministic formulation is made:

$$\begin{array}{lll} \underset{(\mu_{\mathbf{x}},\mathbf{d})}{\text{Minimize}} & \mu_f(\mu_{\mathbf{x}}, \mathbf{d}, \mu_{\mathbf{p}}), & \\ \text{Subject to} & P(g_j(\mathbf{x}, \mathbf{d}, \mathbf{p}) \geq 0) \geq R_j, & j = 1, 2, \ldots, J, \\ & h_k(\mathbf{d}) \geq 0, & k = 1, 2, \ldots, K, \\ & \mathbf{x}^{(L)} \leq \mu_{\mathbf{x}} \leq \mathbf{x}^{(U)}, & \\ & \mathbf{d}^{(L)} \leq \mathbf{d} \leq \mathbf{d}^{(U)}. & \end{array} \tag{2}$$

where μ_f is the function value computed at the mean of variable vector $\mathbf{x}$ and random parameters $\mathbf{p}$. The quantity R_j is the required reliability (within [0,1]) for satisfying j-th constraint. A computational method is used to estimate the probability term $P()$. The above formulation contains all deterministic expressions and hence any existing optimization methodology can be used to solve the problem.

The major difficulty posed by the above problem is to compute the probability, $P()$. The existing reliability-based design optimization procedures can be classified into four classes [1], mainly based on the way the probability term $P()$ is computed:

1. Simulation methods
2. Double-loop methods
3. Decoupled methods, and

4. Single-loop methods

In the following subsections, we describe each of them in some details.

2.1 Simulation Methods

In this procedure, a set of N different solutions can be created by following the known distribution of variation of $\mathbf{x}$ and $\mathbf{p}$. Thereafter, for each sample, each constraint g_j can be evaluated and checked for its violation. If r cases (of N) satisfy all g_j constraints, the probabilistic constraint can be substituted by a deterministic constraint as follows:

$$\frac{r}{N} \geq R. \tag{3}$$

Such a method is simple and works well when the desired reliability R is not very close to one [7, 16]. However, a major bottleneck of this approach is that the sample size N needed for finding r must be of the order of at least $O(1/(1-R))$, such that at least one infeasible case is present in the sample. For a very stringent reliability requirement, such as for a limiting failure probability $(1-R)$ of $O(10^{-6})$, a large sample size ($N \sim O(10^6)$ in the example) is required to compute r. This may be too computationally expensive to be of any practical use. Although better procedures with a biased Monte-Carlo simulation procedure exist [2], the use of reliability techniques [12, 19, 10, 21] to evaluate probabilistic constraints is getting increasingly popular in the recent past, which we discuss next.

2.2 Double-Loop Methods

In the double-loop method, a nested optimization is used. To compute the probability of success of each constraint, an optimization procedure (an inner-level optimization) is used. The outer loop optimizes the original objective function and the inner loop finds an equivalent deterministic version of each probabilistic constraint by formulating and solving an optimization problem. There are two approaches used for this purpose: (i) Performance measure approach (PMA) and (ii) Reliability index approach (RIA). Because of the nested optimization procedures, double-loop methods are computationally expensive.

To find whether a given hard constraint (g_j) is satisfied at a design point, we need to compute the following probability of the complementary failure event:

$$P_j = \int_{g_j(\mathbf{x},\mathbf{d},\mathbf{p})<0} f_{\mathbf{X}}(\mathbf{X}) d\mathbf{X}, \tag{4}$$

where $f_{\mathbf{X}}$ is the joint probability density function of $\mathbf{X} = (\mathbf{x}, \mathbf{p})$. The reliability can be computed as $R_j = 1 - P_j$. It is usually impossible to find an analytical expression for the above integral. Thus, we first convert the $\mathbf{X}$ coordinate system into an independent standard normal coordinate system $\mathbf{U}$, through the Rosenblatt transformation [23]. The standard normal random variables are characterized by zero mean and unit variance. In this space, we approximate the curve ($g_j(\mathbf{x}, \mathbf{d}, \mathbf{p}) = 0$ or equivalently $G_j(\mathbf{U}) = 0$) by a first-order approximation at a suitable point known as the MPP (most probable point) of failure. In other words, the MPP point corresponds to a reliability index β_j, which makes a first-order approximation of $P_j = \Phi(-\beta_j)$, where $\Phi()$ is the standard normal density function. To compute the MPP (or β_j), we have the following two approaches.

2.2.1 Performance Measure Approach (PMA)

To find the MPP in the PMA approach, the following optimization problem is solved:

$$\begin{array}{ll} \text{Minimize} & G_j(\mathbf{U}), \\ \text{Subject to} & \|U\| = \beta_j^r, \end{array} \tag{5}$$

where β_j^r is the required reliability index, computed from the required reliability R_j as follows: $\beta_j^r = \Phi^{-1}(R_j)$. The above formulation finds a $\mathbf{U}^*$ point which lie on a circle of radius β_j^r and makes $G_j(\mathbf{U})$ minimum. The original probability constraint is replaced by

$$G_j(\mathbf{U}^*) \geq 0. \tag{6}$$

Figure 2 illustrates this approach on a hypothetical problem. The figure shows a probabilistic

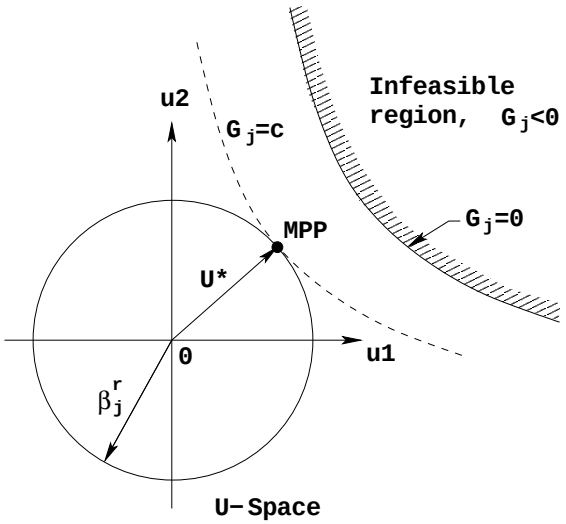

Figure 2: The PMA approach.

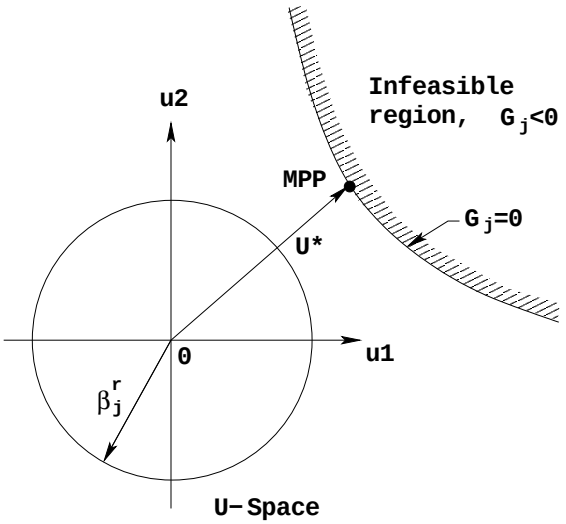

Figure 3: The RIA approach.

constraint g_j into the $\mathbf{U}$-space (for ease of illustration, two variables are considered here). The corresponding constraint $G_j(u_1, u_2)$ and the feasible region are shown. The circle represents $\mathbf{U}$ solutions which corresponds to a reliability index of β_j^r. Thus, the PMA approach finds a point $\mathbf{U}^*$ on the circle for which the function $G_j(\mathbf{U})$ takes the minimum value. Then, if the corresponding constraint function value is non-negative, the probabilistic constraint $P(g_j(\mathbf{x}, \mathbf{d}, \mathbf{p}) \geq 0) \geq R_j$ is considered to have been satisfied.

Although the procedure involves an equality constraint, a special optimization procedure can be used to consider solutions only on the $\|U\| = \beta_j^r$ surface, thereby making every solution a feasible solution. For multiple such probabilistic constraints, ideally the above problem can be solved for each constraint at a time and the minimum of $G_j(\mathbf{U}^*)$ value for all constraints ($j = 1, 2, \ldots, J$) can be used in equation 6. Alternatively, the following non-differentiable objective function can be used to solve the above problem:

$$\begin{array}{ll} \text{Minimize} & \min_{j=1}^{J} G_j(\mathbf{U}), \\ \text{Subject to} & \|U\| = \beta_j^r, \end{array} \tag{7}$$

2.2.2 Reliability Index Approach (RIA)

In this method, the following optimization problem is solved:

$$\begin{array}{ll} \text{Minimize} & \|\mathbf{U}\|, \\ \text{Subject to} & G_j(\mathbf{U}) = 0. \end{array} \tag{8}$$

Here, the MPP is calculated by finding a point which is on the constraint curve in the **U**-space and is nearest to the origin. The optimum point $\mathbf{U}^*$ is used to replace the original probability constraint as follows:

$$\|\mathbf{U}\| \geq \beta_j^r. \tag{9}$$

Figure 3 illustrates the procedure. During the optimization procedure, the desired reliability index β_j^r is ignored and the minimum **U**-vector on the constraint boundary is found. Thereafter, the minimal $\mathbf{U}^*$ is compared with β_j^r.

This approach also involves an equality constraint. Although this method is computationally inferior compared to the PMA approach, a nice aspect is that the optimization problem does not involve the supplied reliability index value. For multiple such constraints, the above procedure can be applied for each constraint and the minimum $\mathbf{U}^*$ can be considered in equation 9. Alternatively, all constraints can be included in the constraint set of equation 8 and the following optimization problem can be solved:

$$\begin{array}{lll} \text{Minimize} & \|\mathbf{U}\|, & \\ \text{Subject to} & G_j(\mathbf{U}) \geq 0, & j = 1, 2, \ldots, J \\ & \Pi_{i=1}^{J} G_j(\mathbf{U}) = 0. & \end{array} \tag{10}$$

The last constraint requires that at least one $G_j(\mathbf{U}) = 0$, thereby finding the constraint j and the corresponding MPP point which is closest to the origin.

2.3 Single-Loop Methods

The single-loop methods [17] combine both optimization tasks together by not exactly finding the optimum of the inner-level optimization task. An approximation procedure is used for the task. As an example, Liang [17] suggested the following replacement of the original probabilistic constraint:

$$g_j(\mathbf{x}, \mathbf{p}, \mathbf{d}) \geq 0, \tag{11}$$

where $\mathbf{x}$ and $\mathbf{p}$ are computed from the derivatives of g_j with respect to $\mathbf{x}$ and $\mathbf{p}$ at the means respectively, as follows:

$$\mathbf{x} = \mu_{\mathbf{X}} - \beta_j^r \sigma \frac{\nabla_{\mathbf{x}} g_j}{\sqrt{\|\nabla_{\mathbf{x}} g_j\|^2 + \|\nabla_{\mathbf{p}} g_j\|^2}}, \tag{12}$$

$$\mathbf{p} = \mu_{\mathbf{p}} - \beta_j^r \sigma \frac{\nabla_{\mathbf{p}} g_j}{\sqrt{\|\nabla_{\mathbf{x}} g_j\|^2 + \|\nabla_{\mathbf{p}} g_j\|^2}}. \tag{13}$$

Since the above is only an approximation to the double-loop procedure, the single-loop methods often cannot produce accurate results, but are computationally quicker than the double-loop methods.

2.4 Decoupled Methods

In the decoupled methods, two optimization (outer and inner-level) approaches are applied one after another in a sequence. Decoupled methods are shown to be the best of the three optimization approaches in a number of recent studies. These methods are started by first finding the best solution in the search space (without considering any uncertainty on design variables $\mathbf{x}$ or parameters $\mathbf{p}$ and using the mean of $\mathbf{x}$ as decision variables). Thereafter, the most-probable point (MPP) for each constraint g_j is found using the PMA or RIA approach. Then in the next iteration, the constraints are shifted according to their MPP points found in the last inner-level optimization. This dual optimization continues in tandem till no further improvement in the current solution is achieved. Figure 4 shows a particular approach (Sequential Optimization and Reliability Assessment (SORA) method) suggested elsewhere [11], in which the PMA approach is used as the second optimization problem.

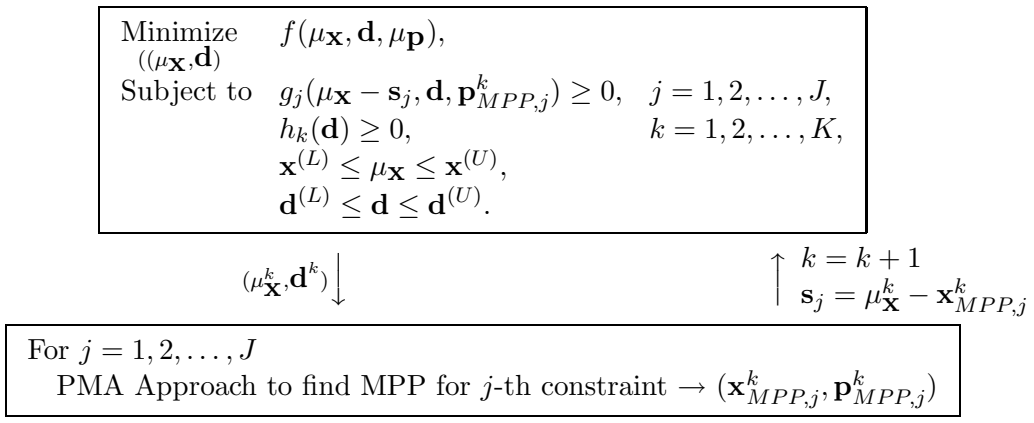

Figure 4: A specific decoupled method (SORA) [11]. Initial value of s_j is set equal to zero for all j.

3 Three Reliability-Based Optimization Cases

Here, we present three different aspects of reliability-based optimization problems which may be difficult to solve using above-mentioned classical optimization techniques, but may have a remedy with an evolutionary optimization algorithm (EA), which constructs a search procedure by mimicking the natural evolutionary principles [15, 13, 4].

3.1 Single-Objective, Multi-Modal Reliability-Based Optimization

Many single-objective optimization problems involve more than one global and local optima. Since most classical methods start with a deterministic optimum, they are likely to begin the reliability-based search procedure from the global optimum. However, in some problems the deterministic global minimum may have such a narrow basin of attraction that the reliable solution (the solution to equation 2) moves far away from the deterministic optimum. On the other hand, the reliability consideration may not move the resulting optimum far away from a deterministic local optimum having a broader basin of attraction. Further, it could be such that the reliable solution for the deterministic global optimum is worse in function value than that for the deterministic local optimum.

In a sufficiently non-linear problem, the reliable minimum (point A' shown in Figure 5) corresponding to the global deterministic minimum (point A) need not be the best solution and the reliable minimum (point B') corresponding to a local deterministic minimum (point B) may be the best. The classical serial procedure of first finding the deterministic global optimum (solution

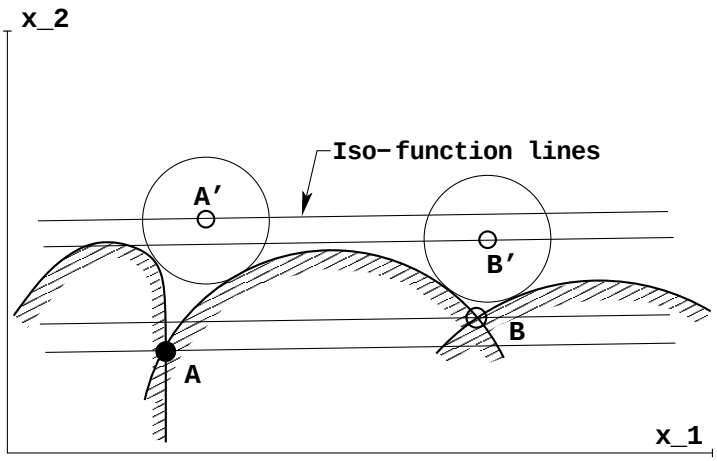

Figure 5: A sketch of two optima A and B and their corresponding reliable solutions (A' and B') for a fixed reliability index.

A) and then finding the reliable solution (solution A') may not be a good idea. Evolutionary optimization methods are population-based approaches and do not need to start its search from a deterministic optimum. They can be directly used to solve the reliability-based optimization problem (equation 2). Moreover, due to their population approach, they are more likely to avoid the locally optimal reliable solution and converge to the true reliable solution.

3.2 Optimization for Seeking Multiple Solutions for Different Reliability Values

In most RBDO studies, the aim is to find the reliable optimum corresponding to a given failure probability (or a given reliability index). However, in the context of design optimization, it would be educative to learn how the reliable solutions change with different levels of reliability index, as shown in Figure 6. When reliability is not considered, the deterministic optimum is the desired solution. As discussed earlier, when the optimization is performed for a particular reliability (say $R = 0.9$), an original feasible (inactive) solution becomes the desired solution. As the reliability value is increased, a different solution somewhat more inside into the feasible region is likely to be the desired solution. That is, if we can locate the reliable optimum for small (say 80%) to large value (say 99.99%) of reliability, it would be worthwhile to analyze the solutions and investigate if they all bring out any common design principles (marked by the solid line connecting the reliable solutions). Such multiple optimal solutions can be deciphered by treating the problem as a two-objective optimization problem of optimizing the original objective and in addition maximize the reliability index (R or β) and by finding a number of Pareto-optimal solutions using an evolutionary multi-objective optimization (EMO) strategy to this bi-objective optimization problem. Such an analysis is likely to provide a plethora of interesting insights about the property of optimal and reliable solutions to a problem at hand. Multiple independent optimization tasks can be eliminated by a single bi-objective optimization task, if a two-objective optimization problem having the original objective function and an additional

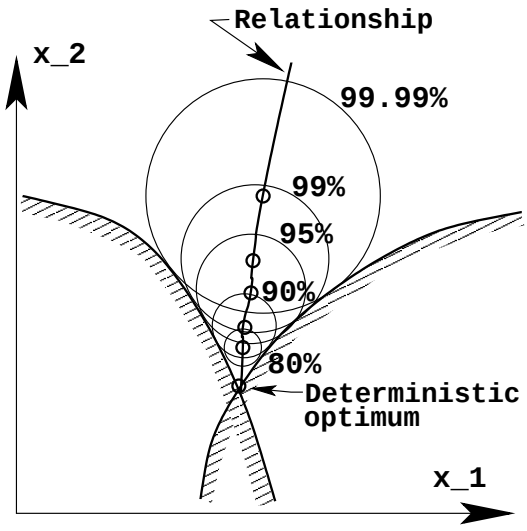

Figure 6: Different reliability index may result in an interesting relationship among reliable solutions.

objective of maximizing reliability R dictated by the solution is formulated and solved:

$$\begin{array}{lll} \underset{(\mu_{\mathbf{X}},\mathbf{d})}{\text{Minimize}} & \mu_f(\mu_{\mathbf{X}},\mathbf{d},\mu_{\mathbf{p}}), & \\ \underset{(\mu_{\mathbf{X}},\mathbf{d})}{\text{Maximize}} & R(\mu_{\mathbf{X}},\mathbf{d},\mu_{\mathbf{p}}) = \min_{i=1}^{J} R_j(\mu_{\mathbf{X}},\mathbf{d},\,\mu_{\mathbf{p}}), & \\ \text{Subject to} & h_k(\mathbf{d}) \geq 0, & k = 1,2,\ldots,K, \\ & \mathbf{x}^{(L)} \leq \mu_{\mathbf{X}} \leq \mathbf{x}^{(U)}, & \\ & \mathbf{d}^{(L)} \leq \mathbf{d} \leq \mathbf{d}^{(U)}. & \end{array} \tag{14}$$

where

$$R_j(\mu_{\mathbf{X}},\mathbf{d},\mu_{\mathbf{p}}) = P(g_j(\mathbf{x},\mathbf{d},\mathbf{p}) \geq 0).$$

The evolutionary multi-objective optimization (EMO) procedure is capable of finding multiple Pareto-optimal solutions for such a bi-objective optimization problem, thereby finding multiple reliable solutions corresponding to differing reliability values. Such a study will help to analyze the effect of reliability index on the quality of solutions (both in objective value and in decision parameter values) and may remain as a method of fixing a suitable reliability index for a particular application.

3.3 Multi-Objective Reliability-Based Optimization

The concept of reliability-based optimization methods can also be applied to solve multi-objective reliability-based optimization problems:

$$\begin{array}{lll} \underset{(\mathbf{x},\mathbf{d})}{\text{Minimize}} & (f_1(\mathbf{x},\mathbf{d},\mathbf{p}),\ldots,f_M(\mathbf{x},\mathbf{d},\mathbf{p})), & \\ \text{Subject to} & g_j(\mathbf{x},\mathbf{d},\mathbf{p}) \geq 0, & j = 1,2,\ldots,J, \\ & h_k(\mathbf{d}) \geq 0, & k = 1,2,\ldots,K, \\ & \mathbf{x}^{(L)} \leq \mathbf{x} \leq \mathbf{x}^{(U)}, & \\ & \mathbf{d}^{(L)} \leq \mathbf{d} \leq \mathbf{d}^{(U)}. & \end{array} \tag{15}$$

In such cases, instead of a single reliable solution, a reliable frontier is the target, as shown in Figure 7. When reliability aspects are considered, the corresponding reliable Pareto-optimal front

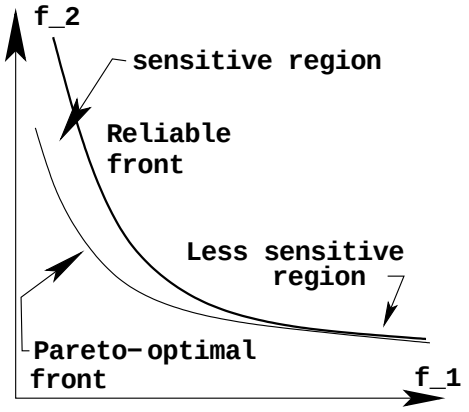

Figure 7: Reliable front in a multi-objective reliability-based optimization problem.

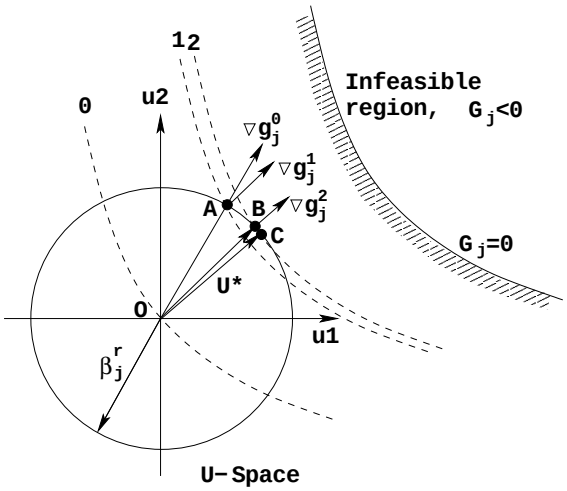

Figure 8: A fast approach for solving the PMA problem.

will be different from the original front and is placed inside the feasible region. As the reliability index is increased (to get more reliable solutions), the front is expected to move further inside the feasible region in the objective space.

An use of EMO procedure can be applied directly on the following deterministic optimization problem:

$$\begin{array}{lll} \underset{(\mu_{\mathbf{X}},\mathbf{d})}{\text{Minimize}} & (\mu_{f_1}(\mu_{\mathbf{X}},\mathbf{d},\mu_{\mathbf{P}}),\ldots,\mu_{f_M}(\mu_{\mathbf{X}},\mathbf{d},\mu_{\mathbf{P}})), & \\ \text{Subject to} & P(g_j(\mathbf{x},\mathbf{d},\mathbf{p})\geq 0)\geq R_j, & j=1,2,\ldots,J, \\ & h_k(\mathbf{d})\geq 0, & k=1,2,\ldots,K, \\ & \mathbf{x}^{(L)}\leq \mu_{\mathbf{X}}\leq \mathbf{x}^{(U)}, & \\ & \mathbf{d}^{(L)}\leq \mathbf{d}\leq \mathbf{d}^{(U)}. & \end{array} \tag{16}$$

The probability constraint $P()$ can handled as before by using any of the four methods. The advantage of finding the complete reliable frontier is that the relative sensitivity of different regions of the frontier can be established with respect to the uncertainties in design variables and parameters. These information will be useful to the designers and decision-makers in choosing a solution from a relatively insensitive region of the trade-off frontier.

There is a fourth problem scenario involving M conflicting objectives, in which an $(M+1)$-dimensional trade-off frontier can be attempted to be found by including an additional objective of maximizing derived reliability R, as considered in subsection 3.2. This will provide a plethora of information about the nature of change of original M-dimensional trade-off frontier with the required reliability value. In this paper, we do not explicitly add such an objective for multi-objective optimization problems, but perform multiple independent M-objective runs with different R values and show the effect of R on the obtained frontier.

4 Proposed Evolutionary Approaches

For the first time, we suggest here reliability-based optimization procedures based on evolutionary optimization algorithms for handling all three problems described above.

For the problems described in subsections 3.1 and 3.3, we suggest a quick procedure of computing the MPP based on the PMA approach. Figure 8 illustrates this procedure. A gradient vector, ∇g_j^0, of each probabilistic constraint g_j is first computed at the origin of the **U**-space. Its intersection (point A) with a circle of radius β_j^r is computed and a new gradient (∇g_j^1) is recomputed at this point (A). Thereafter, the intersection (point B) of this new gradient direction from the origin with the circle is recomputed and a new gradient vector ((∇g_j^2) is computed at B. This procedure is continued till a convergence of the norm of two consecutive gradient vectors with a predefined tolerance (of 0.001) is met. At this point, we have an approximate solution ($\mathbf{U}^*$) to the PMA approach. Such a procedure is already suggested elsewhere [10]. In our approach, we redo the above procedure for each probabilistic constraint and a deterministic constraint is formulated using equation 6. Thereafter, an EA with a penalty-parameter-less constraint handling approach [3] is used to handle all deterministic constraints.

For handling problems described in subsection 3.2, the RIA-based approach is needed. This is because, for every solution it is desired to find the reliability value it corresponds. We use a relatively faster yet an approximate approach here for finding the MPP. First, we find the MPP ($\mathbf{U}^*$) on a *unit-circle* (assuming $\beta_j^r = 1$) based on the above PMA-based fast approach. Thereafter, we perform a uni-directional search along $\mathbf{U}^*$ and locate the point for which $G_j(\mathbf{U}) = 0$. We employ the Newton-Raphson approach for performing the uni-directional search. Here also, we use a tolerance of $\epsilon = 0.001$ for terminating the uni-directional search. Due to a single-variable search employed in the Newton-Raphson search, the computation is usually quick, requiring only a derivative of the constraint function in the **U**-space. However, we recognize here that the MPP point obtained by this procedure need not be the exact solution to the RIA optimization problem, particularly for highly non-linear constraints. More sophisticated methods are in order and research is currently underway in developing such methods.

To find a better search direction $\mathbf{U}^*$, we also suggest another procedure in which we compute the MPP on a circle of radius β_j^r (equal to the desired reliability index), instead of on unit-circle. Since the MPP computation is performed directly on the circle of interest, this approach is expected to produce solutions with better accuracy than the previous approach.

For handling multiple constraints, the above procedure of finding $\mathbf{U}^*$ and then performing the Newton-Raphson method to locate the point on $G_j(\mathbf{U}) = 0$ is repeated for each constraint one at a time. Thus, the inner-level optimization procedure using all design variables needed in the classical double-loop method is replaced by a computationally fast procedure of finding the $\mathbf{U}^*$ direction and then performing a single-variable line search. Such a technique can be employed with a classical optimization procedure or with any other non-classical methods as well. Here, we employ the concept with a multi-objective evolutionary algorithm, namely the elitist non-dominated sorting GA or NSGA-II [6].

In the following sections, we present the problems considered in the study and the results obtained by the proposed methodologies. In the first two cases, we also compare the results with existing decoupled methodologies.

5 Simulation Results on Multi-Modal Reliability-Based Optimization Problems

In a real-world optimization problem, there may exist multiple deterministic optima, each having its own reliable solution. We construct the following two-variable test problem to illustrate one such problem:

$$\left.\begin{array}{ll} \text{Maximize} & y, \\ \text{Subject to} & x^2 - 1000y \geq 0, \\ & y - x + 200 \geq 0, \\ & x - 3y + 400 \geq 0, \\ & -400 \leq x, y \leq 300. \end{array}\right\} \tag{17}$$

In this problem, $\mathbf{x} = (x, y)$ and variables $\mathbf{d}$ are absent and there does not exist any uncertain problem parameter ($\mathbf{p}$). We assume independent and normally distributed uncertainties with $\sigma_1 = \sigma_2 = 10$ and a desired reliability index of 4. We use a real-coded genetic algorithm (GA) along with the PMA approach described above. Tournament selection operator is used to compare two solutions at a time and the better of the two is chosen. Such pair-wise comparisons will create a mating pool containing good solutions. Thereafter, the simulated binary crossover (SBX) operator [5, 4] is used to create two blended offspring solutions using two parent solutions taken at a time from the mating pool. A crossover probability of 0.9, meaning that 90% of the pairs are recombined to create offspring solutions and rest 10% parents are simply chosen, is used. The SBX operator involves a distribution index controlling the spread of obtained solutions. We have used a value of 2, which is recommended in the original study [5]. Finally, a polynomial mutation operator [4] is used to perturb the offspring solutions in their neighborhood. A mutation probability of $1/n$ is used so that on an average one of the design variables are mutated per offspring solution. A distribution index of 50 is used for mutation. For details of these operators, readers may refer to a description given elsewhere [4]. A C-code implementing the above-mentioned GA is available at http://www.iitk.ac.in/kangal/soft.htm. With a population of 30 solutions, the GA procedure is applied for 50 iterations. We find the best solution $(237.908, 11.820)^T$, with a function value of 11.820 (close to solution B'). The minimum, median and worst optimal objective values obtained from 11 runs, each performed from an independent initial population, are found to be 10.694, 11.363, and 11.820, respectively. In all 11 independent runs made by the GA (each starting from a different random initial population), no simulation has converged on or near solution A'. The population-best solutions in every generation are shown in Figure 9 to show how three different GA simulations starting at different region in the search space avoid the local maximum (A') and converge to the global maxima (B'). One of runs has its best located near A' in the initial population and even then the GA with the proposed PMA approach can advance and converge near the global maximum solution.

We have implemented the classical SORA approach [11] discussed in Section 2.4 to solve the above problem. The best solution obtained is $(115.88, -27.55)^T$ with a function value of -27.55 (close to solution A'), which is worse than that found by the GA approach. This is not surprising, because the GA search procedure described above has a global perspective. It is needless to say that the GA-based technique is also capable of solving simpler cases in which the reliable solution corresponding to the globally best deterministic optimum is the best solution. This study clearly indicates the importance of EA-based approaches to difficult reliability-based problem solving tasks.

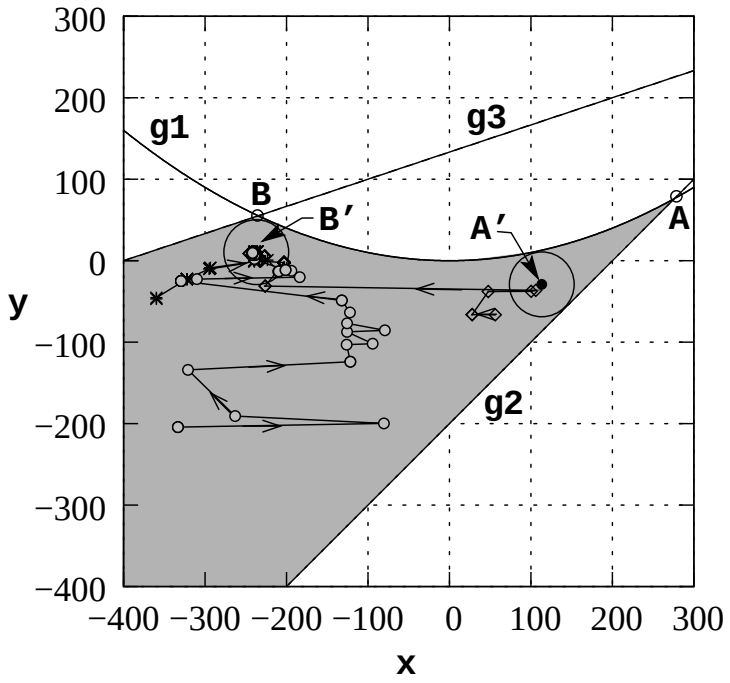

Figure 9: The proceedings of three GA simulations show how population-best solution can progress towards the global maximum (B').

6 Simulation Results for Finding Multiple Reliable Solutions

Here, we consider two problems – a two-variable test problem and an automobile car side-impact problem.

6.1 A Test Problem

First, we consider the following two-variable test problem [1]:

$$\left.\begin{array}{ll} \text{Maximize} & x+y, \\ \text{Subject to} & g_1(x,y) \equiv \frac{1}{20}x^2y - 1 \geq 0, \\ & g_2(x,y) \equiv \frac{1}{30}(x+y-5)^2 + \frac{1}{120}(x-y-12)^2 - 1 \geq 0, \\ & g_3(x,y) \equiv \frac{80}{x^2+8y+5} - 1 \geq 0, \\ & 0 \leq x,y \leq 10. \end{array}\right\} \tag{18}$$

Here, $\mathbf{x} = (x, y)$. To find a set of trade-off optimal solutions, we use the elitist non-dominated sorting GA or NSGA-II [6]. In an NSGA-II, first, the parent population is used to create an offspring solution similar to that in a genetic algorithm, as described earlier. Thereafter, both populations are combined and a sorting of the combined population is performed according to an increasing order of *domination* level. A solution is considered to dominate another solution, if the previous solution is not worse than the latter in all objectives and is better in at least one objective. To construct the population for the next generation, solutions from the top of the sorted list are chosen till solutions from the last front cannot be all accepted to maintain the fixed population size. To decide which all solutions should be chosen, a *niching* strategy is used to choose only those solutions which will make the diversity among them the maximum. This final consideration ensures that a well-diversified set of solutions are found and the emphasis of non-dominated solutions causes a convergence to the Pareto-optimal frontier.

Figure 10 shows the non-dominated solutions obtained by NSGA-II with the proposed MPP-finding strategy (on a unit-circle) with a population size of 100 and run for 100 generations. Values for crossover and mutation indices, as they were chosen in Section 5, are used here. Here, we have

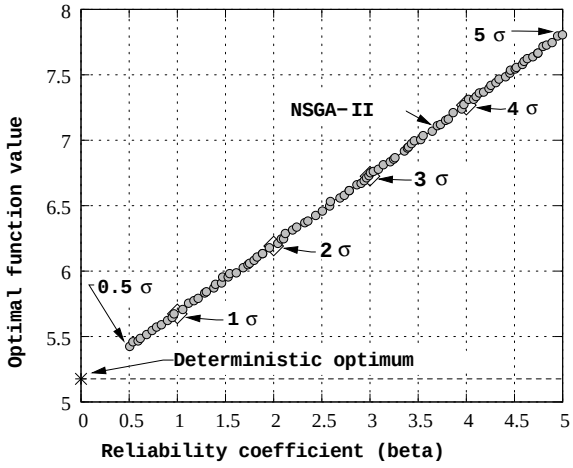

Figure 10: Trade-off frontier between f^* and reliability index β for the two-variable test problem.

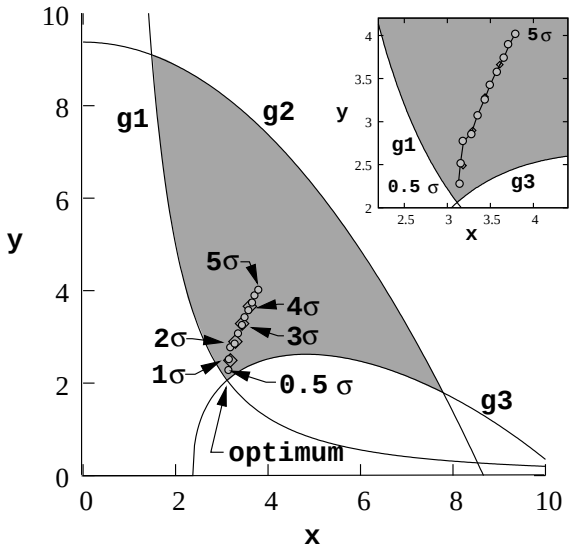

Figure 11: Reliable solutions move inside the feasible region for the two-variable test problem.

restricted the reliability index to vary between 0.5 and 5.0, causing a reliability of 69.14625% to 99.99997%. We have used $\sigma_1 = \sigma_2 = 0.3$ for this problem. It is interesting to note that to achieve a better reliable solution, a compromise of the optimal objective function value must be made. Such a variation of optimal objective value and reliability is important to decision-makers, as this will provide a deeper insight into the trade-off between these two important parameters. When the NSGA-II approach is used with the desired reliability circle (β^r), identical results are obtained.

To investigate whether NSGA-II solutions are optimal, we have solved the same problem with single-objective SORA method – a decoupled method described in Section 2.4 [11] – for different β values, as shown in Table 1. These solutions are also shown in Figure 10 with a 'diamond'. The percentage deviation of NSGA-II results from the SORA results are also tabulated. It can be concluded that NSGA-II with our proposed MPP-finding methodology is able to find solutions close to solutions obtained using SORA.

Figure 11 shows how the optimal solutions move away from the deterministic optimum with an increase in the reliability index. The constraints g_1 and g_3 are active at the deterministic optimum. The inset figure shows that even for $\beta^r = 0.5$, the reliable solution is inside the feasible region (marked shaded). Thereafter, as β^r increases up to 5, the reliable solutions move inside the feasible space. The manner in which the solutions move inside also reveals important insights about the dependency of optimal solutions on the reliability index.

To compare the above results with another MPP-finding algorithm, we consider another state-of-the-art and efficient methodology, which we discuss next.

Table 1: Optimal solutions with different β for the test problem.

β	Optimal f				
	SORA	NSGA-II (unit-circle)		NSGA-II (iHL-RF)	
		f	% dev.	f	% dev.
1	5.673	5.673	0.000	5.676	0.053
2	6.192	6.195	0.048	6.194	0.032
3	6.725	6.752	0.401	6.730	0.074
4	7.268	7.292	0.330	7.273	0.069
5	Not converged	7.806	–	8.146	–

6.2 Classical HL-RF Methodologies

The MPP formulation using the RIA approach for the j-th constraint ($g = G_j$) can be rewritten as follows:

$$\min_{\mathbf{U}} \quad \frac{1}{2}\mathbf{U}^T\mathbf{U}, \tag{19}$$

$$\text{subject to} \quad g(\mathbf{U}) = 0. \tag{20}$$

The family of Hasofer-Lind, Rackwitz-Fiessler (HL-RF) algorithms are based on successive linearization of $g(\mathbf{U})$ [18, 24]. In an improved version of HL-RF method (iHL-RF) [20], following parameters are used: $a, b \in (0,1)$, $\delta > 0$, $\gamma > 0$ and $\epsilon_{tol} > 0$. The basic steps of the iHL-RF algorithm, starting at $k = 0$ from a chosen $\mathbf{U}^k$, are as follows:

1. Find the step $\mathbf{s}^k$ corresponding to a solution for $\mathbf{U}'$ of minimum norm, that solves $g(\mathbf{U}^k) + \nabla_U g[\mathbf{U}' - \mathbf{U}^k] = 0$. This basically corresponds to the solution of Equations 19 and 20 with a linearized version of constraint replacing Equation 20. The step is given by $\mathbf{s}^k = \mathbf{U}' - \mathbf{U}^k$, which can be computed using the minimum norm solution of $\mathbf{U}'$ given by the following equation:

$$\mathbf{U}' = \left[\frac{-\nabla_U g}{\|\nabla_U g\|}\mathbf{U}^k + \frac{g(\mathbf{U}^k)}{\|\nabla_U g\|}\right]\frac{-\nabla_U g^T}{\|\nabla_U g\|}. \tag{21}$$

2. Then, a penalty parameter is computed as follows:

$$\rho^k = \begin{cases} \gamma \max\left[\frac{\|\mathbf{U}^k\|}{\|\nabla_U g\|}, \frac{1}{2}\frac{\|\mathbf{U}^k + \mathbf{s}^k\|^2}{|g(\mathbf{U}^k)|}\right], & \text{if } |g(\mathbf{U}^k)| \geq \delta, \\ \gamma\frac{\|\mathbf{U}^k\|}{\|\nabla_U g\|}, & \text{otherwise.} \end{cases} \tag{22}$$

   The following merit function is used in the iHL-RF procedure:

$$m(\mathbf{U}, \rho) = \frac{1}{2}\mathbf{U}^T\mathbf{U} + \rho|g(\mathbf{U})|. \tag{23}$$

   If $(\nabla_U m(\mathbf{U}^k, \rho^k)\, \mathbf{s}^k) \leq \epsilon_{tol}$ then $\zeta = 1$ and exit, else compute the step-size ζ using a line search based on Armijo's rule, which can be stated as follows:

$$\zeta = \max_j\{[b]^j | m(\mathbf{U}^k + [b]^j\mathbf{s}^k, \rho^k) - m(\mathbf{U}^k, \rho^k) \leq -a[b]^j(\nabla_U m(\mathbf{U}^k, \rho^k)\, \mathbf{s}^k)\}. \tag{24}$$

   where $[b]^j = b \times b \times \ldots (j \text{ times})$. j is initially set to 0 and then j is increased by 1 till the condition in Equation 24 is satisfied. Initial negative values of j can also be set but in the application problems the initial value was set as zero.

3. Find the update $\mathbf{U}^{k+1} = \mathbf{U}^k + \zeta \mathbf{s}^k$, where ζ is the step-size obtained in the earlier step.

4. Convergence check is performed at $\mathbf{U}^{k+1}$. The convergence is achieved if the following convergence is satisfied:

$$\Big(|g(\mathbf{U}^{k+1})| < \epsilon_1\Big) \quad \text{AND} \quad \Big[\Big(\max|\mathbf{s}^k| < 2\epsilon_2\Big) \quad \text{OR} \quad \Big(|(\mathbf{U}^{k+1})^T\mathbf{s}^k| < 2\epsilon_3\Big)\Big]. \qquad (25)$$

where ϵ_1, ϵ_2 and ϵ_3 are preselected tolerances. If the convergence is not achieved, $k = k + 1$ go to Step 1, else exit.

The iHL-RF method is claimed to be globally convergent and computationally efficient, but it has to be noted that it can fail for badly scaled problems because of its dependence on the linearization of g.

6.3 NSGA-II with iHL-RF Strategy

To constitute a search algorithm with iHL-RF strategy, we simply replace our proposed MPP-finding methodology with the above iHL-RF procedure. We use the following iHL-RF parameter values suggested in the original study [20]:

$$\begin{array}{llll} \epsilon_1 = 10^{-7}, & \epsilon_2 = 10^{-3}, & \epsilon_3 = 10^{-3}, & \epsilon_{\text{tot}} = 10^{-9}, \\ \delta = 10^{-6}, & a = 0.1, & b = 0.5, & \gamma = 2. \end{array}$$

Table 1 shows the NSGA-II results with iHL-RF methodology on the two-variable test problem. Although the iHL-RF strategy is able to find slightly better solutions than our approach in this problem, the percentage deviations from the single-objective SORA results are not much, as shown in the table. Figure 12 shows the Pareto-optimal front with the proposed approach of MPP computation on a unit-circle and that obtained with NSGA-II in which MPP computation is made with the iHL-RF procedure. In this problem, both procedures find the same Pareto-

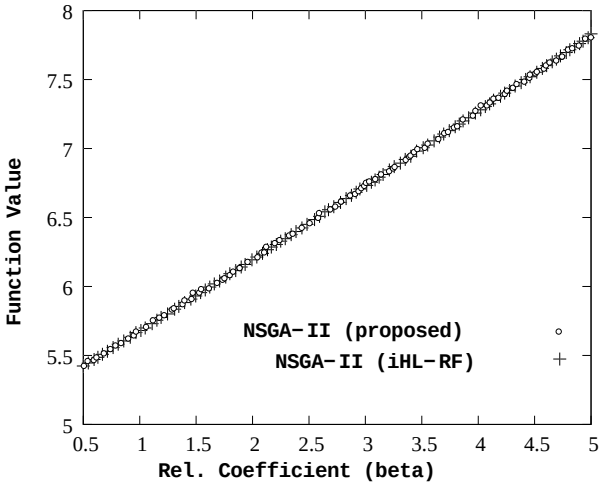

Figure 12: Comparison of NSGA-II with the proposed methodology and iHL-RF method on the two-variable test problem.

optimal front. Next, we consider a car side-impact optimal design problem.

6.4 Car Side-Impact Problem

Next, we consider the car side-impact problem [14]. A car is subjected to a side-impact based on European Enhanced Vehicle-Safety Committee (EEVC) procedures. The effect of the side-impact on a dummy in terms of head injury (HIC), load in abdomen, pubic symphysis force, viscous criterion ($V*C$), and rib deflections at the upper, middle and lower rib locations are considered. The effect on the car are considered in terms of the velocity of the B-Pillar at the middle point and the velocity of the front door at the B-Pillar. An increase in dimension of the car parameters may improve the performance on the dummy, but with a burden of increased weight of the car, which may have an adverse effect on the fuel economy. Thus, there is a need to come up with a design having a balance between the weight and the safety performance. The optimization problem formulated elsewhere [14] included the minimization of the weight of the car subject to EEVC restrictions on safety performance. There are 11 design variables. Their description and the standard deviation of their variations are shown below:

x_1:	Thickness of B-Pillar inner (0.03)	x_6:	Thickness of door beltline reinforcement (0.03)
x_2:	Thickness of B-Pillar reinforcement (0.03)	x_7:	Thickness of roof rail (0.03),
x_3:	Thickness of floor side inner (0.03),	x_8:	Material of B-Pillar inner (0.006),
x_4:	Thickness of cross members (0.03),	x_9:	Material of floor side inner (0.006),
x_5:	Thickness of door beam (0.05),	x_{10}:	Barrier height (10),
		x_{11}:	Barrier hitting position (10).

The NLP formulation is as follows:

$$
\left.
\begin{array}{ll}
\underset{(x_1,\ldots,x_7)}{\text{Minimize}} & f(\mathbf{x}) = \text{Weight}, \\
\text{Subject to} & g_1(\mathbf{x}) \equiv \text{Abdomen load} \le 1 \text{ kN}, \\
& g_2(\mathbf{x}) \equiv V * C_u \le 0.32 \text{ m/s}, \\
& g_3(\mathbf{x}) \equiv V * C_m \le 0.32 \text{ m/s}, \\
& g_4(\mathbf{x}) \equiv V * C_l \le 0.32 \text{ m/s}, \\
& g_5(\mathbf{x}) \equiv D_{ur} \text{ upper rib deflection} \le 32 \text{ mm}, \\
& g_6(\mathbf{x}) \equiv D_{mr} \text{ middle rib deflection} \le 32 \text{ mm}, \\
& g_7(\mathbf{x}) \equiv D_{lr} \text{ lower rib deflection} \le 32 \text{ mm}, \\
& g_8(\mathbf{x}) \equiv F \text{ Pubic force} \le 4 \text{ kN}, \\
& g_9(\mathbf{x}) \equiv V_{MBP} \text{ Velocity of V-Pillar at middle point} \le 9.9 \text{ mm/ms}, \\
& g_{10}(\mathbf{x}) \equiv V_{FD} \text{ Velocity of front door at V-Pillar} \le 15.7 \text{ mm/ms}, \\
& 0.5 \le x_1 \le 1.5, \quad 0.45 \le x_2 \le 1.35, \\
& 0.5 \le x_3 \le 1.5, \quad 0.5 \le x_4 \le 1.5, \\
& 0.875 \le x_5 \le 2.625, \quad 0.4 \le x_6 \le 1.2, \\
& 0.4 \le x_7 \le 1.2.
\end{array}
\right\} \qquad (26)
$$

In this problem, we partition the 11-variable vector $\mathbf{x}$ into two sets: uncertain decision variables $\mathbf{x} = (x_1, \ldots, x_7)$ and uncertain parameters $\mathbf{p} = (x_8, \ldots, x_{11})$. Here, all variables/parameters (in mm) are assumed to be stochastic with a standard deviations (in mm) marked above. Problem parameters x_8 to x_{11} are assumed to take a particular distribution with a fixed mean of 0.345, 0.192, 0, and 0 mm, respectively. Thus, the stochastic optimization problem involves seven decision variables, whereas all 11 quantities vary with normal distribution around their mean values and are assumed to be independent. This functional forms of the objective function and

constraints are given below:

$$
\begin{aligned}
f(\mathbf{x}) &= 1.98 + 4.9x_1 + 6.67x_2 + 6.98x_3 + 4.01x_4 + 1.78x_5 + 0.00001x_6 + 2.73x_7, && (27)\\
g_1(\mathbf{x}) &= 1.16 - 0.3717x_2x_4 - 0.00931x_2x_{10} - 0.484x_3x_9 + 0.01343x_6x_{10}, && (28)\\
g_2(\mathbf{x}) &= 0.261 - 0.0159x_1x_2 - 0.188x_1x_8 - 0.019x_2x_7 + 0.0144x_3x_5 + 0.87570.001x_5x_{10} && (29)\\
&\quad +0.08045x_6x_9 + 0.00139x_8x_{11} + 0.00001575x_{10}x_{11}, && (30)\\
g_3(\mathbf{x}) &= 0.214 + 0.00817x_5 - 0.131x_1x_8 - 0.0704x_1x_9 + 0.03099x_2x_6 - 0.018x_2x_7 + 0.0208x_3x_8 && (31)\\
&\quad +0.121x_3x_9 - 0.00364x_5x_6 + 0.0007715x_5x_{10} - 0.0005354x_6x_{10} + 0.00121x_8x_{11} + && (32)\\
&\quad 0.00184x_9x_{10} - 0.018x_2x_2, && (33)\\
g_4(\mathbf{x}) &= 0.74 - 0.61x_2 - 0.163x_3x_8 + 0.001232x_3x_{10} - 0.166x_7x_9 + 0.227x_2x_2, && (34)\\
g_5(\mathbf{x}) &= 28.98 + 3.818x_3 - 4.2x_1x_2 + 0.0207x_5x_{10} + 6.63x_6x_9 - 7.77x_7x_8 + 0.32x_9x_{10}, && (35)\\
g_6(\mathbf{x}) &= 33.86 + 2.95x_3 + 0.1792x_{10} - 5.057x_1x_2 - 11x_2x_8 - 0.0215x_5x_{10} - 9.98x_7x_8 + 22x_8x_9, && (36)\\
g_7(\mathbf{x}) &= 46.36 - 9.9x_2 - 12.9x_1x_8 + 0.1107x_3x_{10}, && (37)\\
g_8(\mathbf{x}) &= 4.72 - 0.5x_4 - 0.19x_2x_3 - 0.0122x_4x_{10} + 0.009325x_6x_{10} + 0.000191x_{11}x_{11}, && (38)\\
g_9(\mathbf{x}) &= 10.58 - 0.674x_1x_2 - 1.95x_2x_8 + 0.02054x_3x_{10} - 0.0198x_4x_{10} + 0.028x_6x_{10}, && (39)\\
g_{10}(\mathbf{x}) &= 16.45 - 0.489x_3x_7 - 0.843x_5x_6 + 0.0432x_9x_{10} - 0.0556x_9x_{11} - 0.000786x_{11}x_{11}. && (40)
\end{aligned}
$$

We use a population of size 100 and run NSGA-II to optimize two objectives $f(x)$ and R for 100 generations. Figure 13 shows the trade-off between f^* and R. Here, we restricted β to

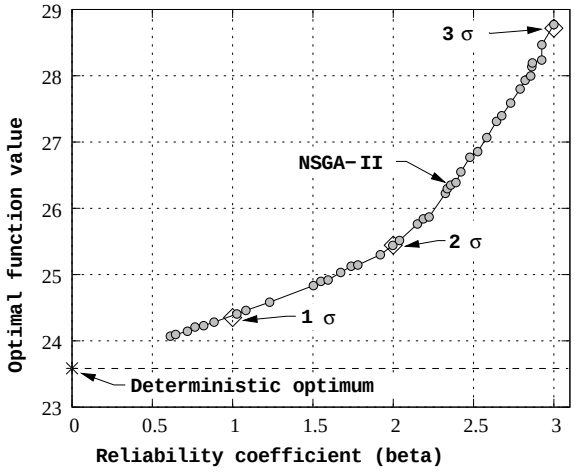

Figure 13: Trade-off frontier between f^* and reliability index β for the car side-impact problem.

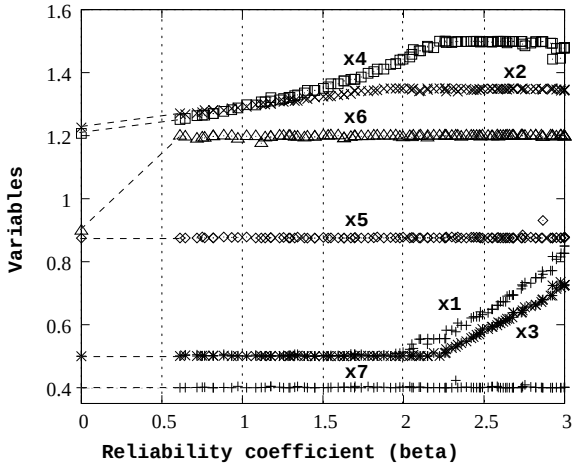

Figure 14: Reliable solutions move inside the feasible region for the car side-impact problem.

vary between 0.5 and 3 (reliability of 99.865%). The corresponding SORA solutions (presented in Table 2 and marked with 'diamonds' in Figure 14) confirm the near-optimality of the obtained solutions. Interestingly, in this problem, a larger than linear sacrifice in f^* needs to be made for an increase in β. The deterministic minimum (f^*) – without any variation in variables – is also shown in the figure.

Figure 14 shows how all seven variables vary with the reliability coefficient. Interestingly, x_5, x_6 and x_7 remains fixed for all reliable solutions. Variables x_5 and x_7 are fixed at their lower bounds and x_6 gets fixed at its upper bound. The optimal strategy in all solutions seems to use the smallest dimension for thickness of door beam (x_5) and roof rail (x_7) and the largest possible dimension for the door beltline reinforcement (x_6). For solutions up to around $\beta = 2$

Table 2: NSGA-II solutions (final three columns) for car side-impact problem are compared with SORA.

β	Optimal Objective Value			
	SORA	Unit circle	Rel. circle	iHL-RF
1	24.352	24.360	24.330	25.357
2	25.443	25.415	25.330	25.476
3	28.718	28.520	28.210	29.708

(corresponding to 97.725% reliability), x_1 and x_3 remain fixed to their lower bounds and thereafter they increase with reliability. These variables represent the thickness of B-Pillar inner and floor side inner, respectively. On the other hand, till about this critical reliability requirement, x_2 (thickness of B-Pillar reinforcement) and x_4 (thickness of cross members) take large values and increase with reliability. After a critical reliability index, these values get fixed to their allowed upper limit.

Thus, overall it seems that a good recipe to obtain an optimal yet reliable solution is to make the reinforcements stronger, while compromising the weight by using thinner members of other components. The figure also reveals that if no upper bound is used for these variables, the optimal strategy would be to use a monotonically increased dimension of x_2 and x_4 with increased reliability requirement. Since an upper limit was used, when the variables reach their upper limits, the optimal way to increase the reliability of the car is to use thicker members for B-Pillar inner (x_1) and floor side inner (x_3). Such information about the nature of solutions and their interactions with the reliability index are interesting and provide valuable knowledge about the problem to a design engineer. Such an analysis procedure for finding useful information about a problem via a multi-objective optimization task is termed as an *innovization* task in a recent study [8]. Here, we show a higher-level concept of the innovization task in which salient relationship among *reliable* trade-off solutions are revealed.

Identical parameters to those used in the previous test problem are chosen here for the iHL-RF study. Figure 15 plots the Pareto-optimal fronts for the proposed method with MPP computation at unit-circle, at desired reliability circle and with iHL-RF algorithm. Table 2 also tabulates the optimum function values at some specific reliability values. It is interesting to note that the difference in the three procedures is more for more stringent reliability consideration. Since MPP computation is more accurate at the desired reliability circle, the optimal function value is found to be better for this case compared to the unit-circle case. However, both proposed methods out-perform the iHL-RF procedure implemented with the specific parameter settings used in this study. A more rigorous parametric study on the iHL-RF method may be necessary to make a more reliable conclusion about the superiority of proposed methodologies over iHL-RF method. Nevertheless, this detail study shows the usefulness of the proposed procedure even in a real-world optimization problem.

7 Simulation Results on Multi-Objective Reliability-Based Optimization Problems

Finally, we consider a couple of two-objective optimization problems to illustrate the effect of considering reliability in multi-objective optimization.

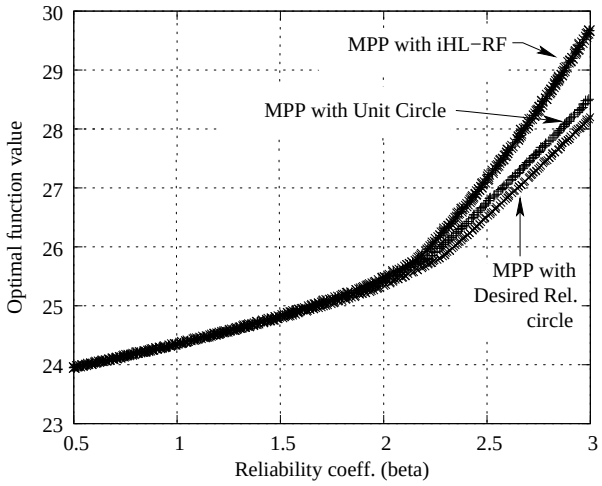

Figure 15: Comparison of NSGA-II with both proposed methods and iHL-RF method on the car side-impact problem.

7.1 A Test Problem

First, we solve a two-variable, two-objective test problem [4]:

$$\left.\begin{array}{ll} \text{Maximize} & x, \\ \text{Maximize} & \frac{1+y}{x}, \\ \text{Subject to} & y + 9x - 6 \geq 0, \\ & -y + 9x - 1 \geq 0, \\ & 0.1 \leq x \leq 1, \quad 0 \leq y \leq 5. \end{array}\right\} \tag{41}$$

Both variables are uncertain: $\mathbf{x} = (x, y)$ with $\sigma = 0.03$. We use a population of size 50 and run NSGA-II till 50 generations. Figure 16 shows the deterministic front and three reliable frontiers with β equal to 1.28 (90%), 2 (97.725%) and 3 (99.875%), respectively. A part of the

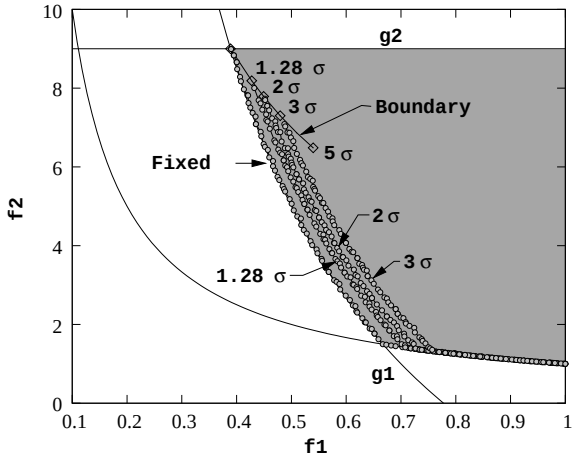

Figure 16: Trade-off frontiers between f_1 and f_2 for different β for the two-constraint test problem.

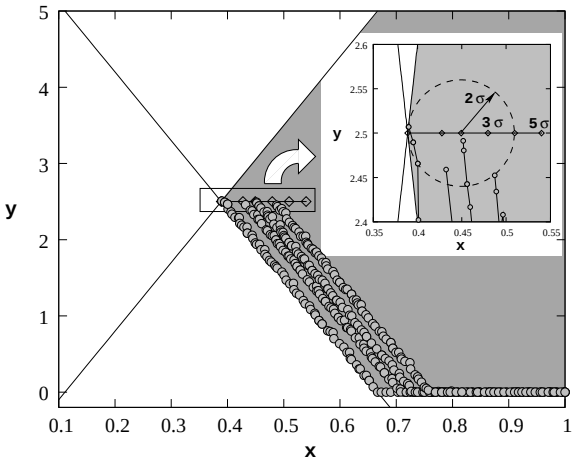

Figure 17: Corresponding reliable solutions for the two-constraint test problem.

deterministic front lies on constraint g_1 and the minimum f_1 solution lies also on constraint g_2. The figure shows how the optimal trade-off frontier moves inside the feasible objective space with an increase in β. For $\beta > 0$, both constraints govern the location of the reliable trade-off frontier. The theoretical change in the minimum f_1 solution is marked ('Boundary'). The figure indicates that optimal solutions for small f_2 are more reliable and less vulnerable to change due to reliability consideration than the small f_1 solutions.

Figure 17 supports this argument. The figure shows how the solutions get inside the feasible region with an increase in β. To be safe from both constraints, the minimum f_1 solution must be moved equally away from both of them, as shown in the inset figure. The circle indicates that the case in which the $\beta = 2$ variation boundary touches both constraints.

7.2 Two-Objective Car Side-Impact Problem Revisited

We use the car side-impact problem discussed earlier, but now use an additional objective of minimizing the average rib deflection, calculated by taking the average of three deflections $g_5(\mathbf{x})$, $g_6(\mathbf{x})$ and $g_7(\mathbf{x})$. All 10 constraints are considered. Figure 18 shows the reliable front as a function of β. Once again, with an increase in the reliability index, the optimal frontier gets worse. We

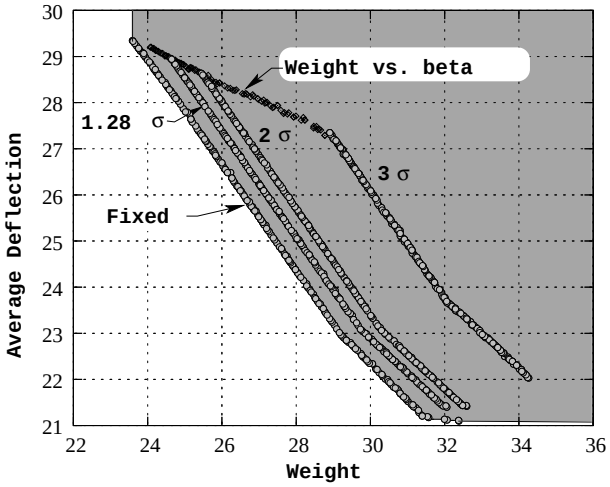

Figure 18: Trade-off frontiers between f_1 and f_2 for different β for the car side-impact problem.

observe the following features from the figure:

- The figure indicates the rate at which the front deteriorates. In this problem, the rate of deterioration seems to be faster than linear, as was also discussed in Section 6.4. Thus, an unnecessary large reliability index corresponds to solutions which are far from being optimum. Designers must carefully set a reliability index to make a good compromise on the optimality of solutions.

- An interesting fact about this problem is that the front moves inside the feasible objective space parallel to each other, indicating that the whole front is uniformly sensitive to a change in the reliability index.

- The minimum-weight solutions are found to be sensitive to the chosen reliability index. The optimal solutions obtained in Figure 14 in Section 6.4 are also plotted in Figure 19 (marked as 'Weight vs. beta'). Interestingly, these solutions mark the boundary to the obtained NSGA-II solutions of this section. This fact provides confidence in the accuracy of the obtained solutions.

Figure 19 shows the variation of design variables for the solutions of the reliable frontier with $\beta = 2$. It is interesting to note that the optimal way to have the trade-off between the weight and

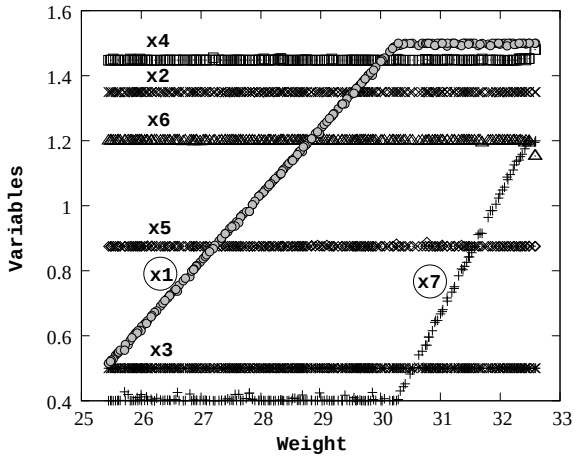

Figure 19: Reliable solutions corresponding trade-off frontiers for $\beta = 2$ in the car side-impact problem.

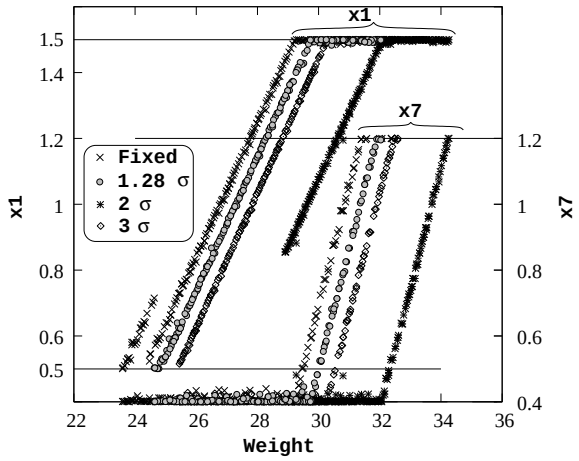

Figure 20: Variables x_1 and x_7 for different β values.

rib-deflection is to have changes in variables x_1 (thickness of B-Pillar inner) and x_7 (thickness of roof rail). All other variables remain fixed to either their lower or their upper bounds. The minimum weight solution corresponds to the lowest allowable values of x_1 and x_7, as were found in section 6.4. For better rib-deflection solutions, the thickness of B-Pillar inner (x_1) must be increased steadily. When its value reaches its upper limit (1.5 mm), the thickness of roof rail (x_7) must be increased by keeping x_1 at its upper limit. The kink in the Pareto-optimal front occurs when x_1 hits its upper bound. Since a different pattern in the variables (now x_1 is kept fixed and x_7 is increased), the Pareto-optimal behavior changes. Figure 20 shows variation of x_1 and x_7 for cases with different β values. In all cases, a similar pattern of changes in these two variables is observed.

Such a study also indicates the differential sensitivities of Pareto-optimal solutions, a matter which is useful for designers and practitioners to make a better multi-criterion decision-making by concentrating on the portion of the Pareto-optimal front which is less sensitive to design variable and parameter uncertainties.

8 Conclusions

In this paper, we have reviewed the recent classical probabilistic methods for handling uncertainties in arriving at reliable solutions, instead of optimal solutions, in an optimization problem. By reviewing these methodologies, we have identified at least three different problem domains in which the classical reliability-based optimization approaches may not be found adequate. The problems have complexities – multi-modality and multi-objectiveness – which are difficult to handle using a classical point-by-point approach. Here, we have developed a couple of evolutionary optimization based approaches for handling probabilistic constraints under uncertainties in decision variables and/or problem parameters to solve the problems to satisfaction. On a number of test problems and an automobile design problem, the proposed procedures have shown their efficacy in quickly finding the desired reliable solution(s). In the car side-impact design problem, a number of interesting properties about the optimal solutions have been revealed. The proposed

evolutionary methods are compared with two state-of-the-art classical methodologies and the niche of the former in single and multi-objective reliability-based optimization has been clearly demonstrated. This study should encourage researchers and practitioners in the area of classical reliability-based design optimization to pay more attention to EA-based search and optimization procedures and vice versa, a process which may lead to the development of more such hybrid evolutionary-classical RBDO approaches in the coming years.

Acknowledgments

The authors acknowledge the funding from India Science Laboratory (ISL), General Motors R&D, Bangalore for executing the study.

References

[1] H. Agarwal. *Reliability based design optimization: Formulations and Methodologies*. PhD thesis, University of Notre Dame, 2004.

[2] T. R. Cruse. *Reliability-based mechanical design*. New York: Marcel Dekker, 1997.

[3] K. Deb. An efficient constraint handling method for genetic algorithms. *Computer Methods in Applied Mechanics and Engineering*, 186(2–4):311–338, 2000.

[4] K. Deb. *Multi-objective optimization using evolutionary algorithms*. Chichester, UK: Wiley, 2001.

[5] K. Deb and R. B. Agrawal. Simulated binary crossover for continuous search space. *Complex Systems*, 9(2):115–148, 1995.

[6] K. Deb, S. Agrawal, A. Pratap, and T. Meyarivan. A fast and elitist multi-objective genetic algorithm: NSGA-II. *IEEE Transactions on Evolutionary Computation*, 6(2):182–197, 2002.

[7] K. Deb and P. Chakroborty. Time scheduling of transit systems with transfer considerations using genetic algorithms. *Evolutionary Computation Journal*, 6(1):1–24, 1998.

[8] K. Deb and A. Srinivasan. Innovization: Innovating design principles through optimization. In *Proceedings of the Genetic and Evolutionary Computation Conference (GECCO-2006)*, pages 1629–1636, New York: The Association of Computing Machinery (ACM), 2006.

[9] O. Ditlevsen and H. O. Madsen. *Structural Reliability Methods*. New York: Wiley, 1996.

[10] X. Du and W. Chen. A most probable point based method for uncertainty analysis. *Journal of Design and Manufacturing Automation*, 4:47–66, 2001.

[11] X. Du and W. Chen. Sequential optimization and reliability assessment method for efficient probabilistic design. *ASME Transactions on Journal of Mechanical Design*, 126(2):225–233, 2004.

[12] X. Du, A. Sudjianto, and W. Chen. An integrated framework for optimization using inverse reliability strategy. *ASME Transactions on Journal of Mechanical Design*, 126(4):562–570, 2004.

[13] D. E. Goldberg. *Genetic Algorithms for Search, Optimization, and Machine Learning*. Reading, MA: Addison-Wesley, 1989.

[14] L. Gu, R. J. Yang, C. H. Tho, L. Makowski, O. Faruque, and Y. Li. Optimization and robustness for crashworthiness of side impact. *International Journal of Vehicle Design*, 26(4), 2001.

[15] J. H. Holland. *Adaptation in Natural and Artificial Systems.* Ann Arbor, MI: MIT Press, 1975.

[16] R. T. F. King, H. C. S. Rughooputh, and K. Deb. Evolutionary multi-objective environmental/economic dispatch: Stochastic versus deterministic approaches. In *Proceedings of the Third International Conference on Evolutionary Multi-Criterion Optimization (EMO-2005)*, pages 677–691. Lecture Notes on Computer Science 3410, 2005.

[17] J. Liang, Z. Mourelatos, and J. Tu. A single loop method for reliability based design optimization. In *Proceedings of the ASME Design Engineering Technical Conferences*, 2004.

[18] P. L. Liu and A. Der Kiureghian. Optimization algorithms for structural reliability. *Structural Safety*, 9:161–177, 1991.

[19] S. Mahadevan and A. Chiralaksanakul. Reliability-based design optimization methods. In *Proceedings of the ASME Design Engineering Technical Conferences DETC2004-57456*, 2004.

[20] D. Padmanabhan. *Reliability based optimization for multidisciplinary system design.* PhD thesis, Department of Mechanical Engineering, University of Notre Dame, Indiana, 2003.

[21] D. Padmanabhan and S. M. Batill. Reliability based optimization using approximations with applications to multi-disciplinary system design. In *Proceedings of the 40th AIAA Sciences & Exhibit,* AIAA-2002-0449, 2002.

[22] S. S. Rao. Genetic algorithmic approach for multiobjective optimization of structures. In *Proceedings of the ASME Annual Winter Meeting on Structures and Controls Optimization*, volume 38, pages 29–38, 1993.

[23] M. Rosenblatt. Remarks on a multivariate transformation. *Annals of Mathematical Statistics*, 23:470–472, 1952.

[24] Y. Zhang and A. Der Kiureghian. Finite element reliability methods for inelastic structures. Technical Report NSF Report UCB/SEMM-97/05, Department of Civil and Environmental Engg., Univ.of California, Berkeley, 1997.